Short communication

On the sensitivity of third-order Volterra MVDR beamformers to interference-pulse shaping filter

Jean-Pierre Delmas [a],*, Pascal Chevalier [b,c], Mustapha Sadok [d]

[a] Samovar CNRS, Telecom SudParis, Institut Polytechnique de Paris, Evry Cedex 91011, France
[b] CNAM, CEDRIC Laboratory, Hesam University, 292 rue Saint-Martin, Paris Cédex 3 75141, France
[c] Thales HTE/AMS/TCP, 4 Av. des Louvresses, Gennevilliers 92622, France
[d] Institut National des Télécommunications et TIC, LaRATIC, Oran, Algeria

ARTICLE INFO

ABSTRACT

Linear beamformers are optimal, in a mean square (MS) sense, when the signal of interest (SOI) and observations are jointly Gaussian and circular. Otherwise, optimal beamformers become non-linear with a structure depending on the unknown joint probability distribution of the SOI and observations. In this context, third-order Volterra minimum variance distortionless response (MVDR) beamformers have been proposed recently to improve the performance of linear beamformers in the presence of non-Gaussian and potentially non-circular interference, omnipresent in practical situations. High performance gains have been obtained for binary phase shift keying (BPSK) and quadrature phase shift keying (QPSK) interference having a square pulse shaping filter in particular. However in practice, for spectral efficiency reasons, most of signals use non-square pulse shaping filters, such as square root raised cosine filter. It is then important to analyze the sensitivity of third-order MVDR beamformers to interference pulse shaping filter, which is the purpose of this paper.

© 2019 Elsevier B.V. All rights reserved.

1. Introduction

Beamforming plays an important role in many applications such as radar, sonar, satellite communications, radiocommunications, acoustic or spectrum monitoring [1]. It allows to optimize, by a linear filtering of the observations, the reception of a SOI potentially corrupted by interference. The most popular receive beamformer has been introduced by Capon et al. [2] at the end of the sixties and corresponds to the MVDR beamformer. Its implementation only requires the a priori knowledge or estimation of the steering vector of the SOI, hence its great interest for spectrum monitoring or passive listening in particular. It corresponds to a particular case of linearly constrained minimum variance (LCMV) beamformer [3] whose equivalent unconstrained form is the generalized sidelobe canceller (GSC) introduced in [4].

Nevertheless it is now well-known [5] that the optimal beamformer, in a MS sense, whose output corresponds to the conditional expectation of the SOI with respect to the observations, is linear only when the SOI and the observations are jointly Gaussian and circular [6]. When the SOI and observations are zero-mean, jointly Gaussian but non-circular, the optimal beamformer becomes WL [5]. For this reason, several WL MVDR [7–9] and WL MMSE [9,10] beamformers have been introduced recently to improve the performance of Capon beamformer for SO non-circular interference. In the more general case of non-Gaussian observations, omnipresent in practice, optimal beamformers become non-linear with a structure depending on the unknown joint probability distribution of the SOI and observations. In this context, third-order Volterra MVDR beamformers have been proposed recently [11] for small-scale systems, to improve the performance of Capon beamformer in the presence of non-Gaussian and potentially non-circular interference, omnipresent in practical situations. High performance gains have been reported for Bernoulli-based impulsive interference and for BPSK and QPSK interference having a square pulse shaping filter in particular. However in practice, for spectral efficiency reasons, most of signals use non-square pulse shaping filters, such as square root raised cosine filter. It then becomes important to analyze the sensitivity of third-order MVDR beamformers to interference pulse shaping filter, which is the purpose of the paper.

* Corresponding author.
E-mail addresses: jean-pierre.delmas@it-sudparis.eu (J.-P. Delmas), pascal.chevalier@cnam.fr (P. Chevalier), msadok@inttic.dz (M. Sadok).

Section 2 introduces the observation model, recalls the structure and implementation of the third-order Volterra MVDR beamformers introduced in [11] and formulates the problem addressed in this paper. Section 3 presents, for a discrete time implementation of the previous beamformers, the asymptotic second order (SO), fourth order (FO) and sixth order (SIO) time-averaged statistics of an interference having an arbitrary pulse shaping filter. Sections 4 and 5 analyze the impact of the interference pulse shaping filter on the steady state and finite samples performance of the third-order Volterra MVDR beamformers respectively. Finally, Section 6 concludes this paper.

The following notations are used throughout the paper. Matrices and vectors are represented by bold upper case and bold lower case characters, respectively. Vectors are by default in column orientation, while T, H and $*$ stand for transpose, conjugate transpose and conjugate, respectively. $E(.)$ is the expectation operator. $\text{Diag}(\mathbf{A}_1, \ldots, \mathbf{A}_q)$ represents a block diagonal matrix of diagonal elements $\mathbf{A}_1, \ldots, \mathbf{A}_q$. $\otimes$ denotes the Kronecker product and $\mathbf{A}^{\otimes q}$ means $\mathbf{A} \otimes \mathbf{A} \ldots \otimes \mathbf{A}$ with $q-1$ Kronecker products.

2. Observation model, third order Volterra MVDR beamformers and problem formulation

2.1. Observation model

We consider an array of N narrowband sensors and we denote by $\mathbf{x}(t)$ the vector of the complex amplitudes of the signals at the output of these sensors. Each sensor is assumed to receive the contribution of an SOI corrupted by a digitally and linearly modulated interference, omnipresent in the context of spectrum monitoring of radiocommunications networks in particular, and a background noise. Under these assumptions, the $N \times 1$ observation vector $\mathbf{x}(t)$ can be written as follows

$$\mathbf{x}(t) = s(t)\mathbf{s} + \mu e^{i\phi} \sum_k a_k v(t - kT - \tau)\mathbf{j} + \mathbf{e}(t) \stackrel{\text{def}}{=} s(t)\mathbf{s} + j(t)\mathbf{j}$$
$$+ \mathbf{e}(t) \stackrel{\text{def}}{=} s(t)\mathbf{s} + \mathbf{n}(t) \in \mathbb{C}^N. \qquad (1)$$

Here, $s(t)$ and $\mathbf{s}$ correspond to the complex envelope, assumed zero-mean, and the steering vector, assumed perfectly known, of the SOI respectively. The a_k's are i.i.d. zero-mean random variables corresponding to the symbols of the interference, T is the symbol duration, $\tau \in [0, T)$ is the initial sampling time, $v(t)$ is a receive real-valued pulse shaping filter, μ and ϕ are constants controlling the amplitude and phase of the interference of unknown steering vector $\mathbf{j}$, respectively. The vector $\mathbf{e}(t)$ is the background noise vector assumed to be zero-mean, stationary, Gaussian circular and spatially white, whereas the vector $\mathbf{n}(t)$ is the total noise vector, containing the background noise and the interference. The SOI, the interference and the background noise are assumed to be statistically independent to each other.

2.2. Third-order Volterra MVDR beamformers

2.2.1. Presentation

We briefly recall the principle and structure of the third order Volterra MVDR beamformers introduced in [11]. These beamformers consist in estimating $s(t)$ from $\mathbf{x}(t)$ without any knowledge on the distribution of $s(t)$ and $\mathbf{n}(t)$. The optimal estimate of $s(t)$ in a mean square (MS) sense from $\mathbf{x}(t)$ is the conditional expectation of $s(t)$ with respect to $\mathbf{x}(t)$, defined by $\hat{s}_{\text{MMSE}}(t) = E[s(t)/\mathbf{x}(t)]$. which requires the knowledge of the probability distribution of $(s(t), \mathbf{x}(t))$ or $(s(t), \mathbf{n}(t))$. As the latter is generally unknown in practice, sub-optimal approaches must be considered. One such approach, exploiting the probability distribution of $\mathbf{n}(t)$ only, consists in considering the beamformer generating the minimum variance

(MV) estimate of $s(t)$ with no distorsion, called MVDR beamformer. This beamformer is generally a non-linear function of $\mathbf{x}(t)$ depending on the probability distribution of the total noise only. As this distribution is unknown in practice, we have proposed in [11] to approximate this MVDR beamformer by third-order Volterra MVDR beamformers. The output of a third-order Volterra beamformer is defined by

$$y(t) = \mathbf{w}_{1,0}^H \mathbf{x}(t) + \mathbf{w}_{1,1}^H \mathbf{x}^*(t) + \mathbf{w}_{3,0}^H [\mathbf{x}(t) \otimes \mathbf{x}(t) \otimes \mathbf{x}(t)]$$
$$+ \mathbf{w}_{3,1}^H [\mathbf{x}(t) \otimes \mathbf{x}(t) \otimes \mathbf{x}^*(t)]$$
$$+ \mathbf{w}_{3,2}^H [\mathbf{x}(t) \otimes \mathbf{x}^*(t) \otimes \mathbf{x}^*(t)]$$
$$+ \mathbf{w}_{3,3}^H [\mathbf{x}^*(t) \otimes \mathbf{x}^*(t) \otimes \mathbf{x}^*(t)] \stackrel{\text{def}}{=} \widetilde{\mathbf{w}}^H \widetilde{\mathbf{x}}(t). \qquad (2)$$

Here, $\mathbf{w}_{1,0}$ and $\mathbf{w}_{1,1}$ are $N \times 1$ spatial filters and $\mathbf{w}_{3,q}$ $(0 \le q \le 3)$ are $N^3 \times 1$ spatial filters, and $\widetilde{\mathbf{x}}(t)$ and $\widetilde{\mathbf{w}}$ are $(2N + 4N^3) \times 1$ vectors defined by $\widetilde{\mathbf{x}}(t) \stackrel{\text{def}}{=} [\mathbf{x}^T(t), \mathbf{x}^H(t), (\mathbf{x}(t) \otimes \mathbf{x}(t) \otimes \mathbf{x}(t))^T, (\mathbf{x}(t) \otimes \mathbf{x}(t) \otimes \mathbf{x}^*(t))^T, (\mathbf{x}(t) \otimes \mathbf{x}^*(t) \otimes \mathbf{x}^*(t))^T, (\mathbf{x}^*(t) \otimes \mathbf{x}^*(t) \otimes \mathbf{x}^*(t))^T]^T$ and $\widetilde{\mathbf{w}} \stackrel{\text{def}}{=} [\mathbf{w}_{1,0}^T, \mathbf{w}_{1,1}^T, \mathbf{w}_{3,0}^T, \mathbf{w}_{3,1}^T, \mathbf{w}_{3,2}^T, \mathbf{w}_{3,3}^T]^T$, respectively. Expression (2) defines in fact the output of several beamformers depending on the potential zero or non-zero values of some spatial filters. In the presence of r cubic terms $(1 \le r \le 4)$ having the index q_j $(1 \le j \le r)$, $(0 \le q_j \le 3)$, the beamformer (2) is called L-C$(q_1, q_2, \ldots, q_r)$ if the first order part is linear or WL-C$(q_1, q_2, \ldots, q_r)$ if the first order part is WL.

To impose no distorsion on $s(t)$ at the output $y(t)$, a set of linear constraints on $\widetilde{\mathbf{w}}$, on the form $\mathbf{C}^H \widetilde{\mathbf{w}} = \mathbf{f}$, has been imposed in [11], where $\mathbf{C}$ is a $(2N + 4N^3) \times (2 + 4[N^3 - (N-1)^3])$ matrix and $\mathbf{f} = (1, \mathbf{0}_{1+4[N^3-(N-1)^3]}^T)^T$. Note that for arbitrary L-C$(q_1, q_2, \ldots, q_r)$ or WL-C$(q_1, q_2, \ldots, q_r)$ beamformers, the dimensions of $\mathbf{C}$, $\widetilde{\mathbf{w}}$ and $\mathbf{f}$ are adjusted accordingly. The best SO estimate (2) of the SOI $s(t)$ exploiting the noise statistics only, thus corresponds to the output of the third-order Volterra beamformer $\widetilde{\mathbf{w}}_{\text{MVDR}}$ which minimizes the time-averaged output power, $\widetilde{\mathbf{w}}^H \mathbf{R}_{\widetilde{x}} \widetilde{\mathbf{w}}$ under the previous constraint,

$$\widetilde{\mathbf{w}}_{\text{MVDR}} = \arg \left\{ \min_{\mathbf{C}^H \widetilde{\mathbf{w}} = \mathbf{f}} \widetilde{\mathbf{w}}^H \mathbf{R}_{\widetilde{x}} \widetilde{\mathbf{w}} \right\}. \qquad (3)$$

where $\mathbf{R}_{\widetilde{x}} \stackrel{\text{def}}{=} <E[\widetilde{\mathbf{x}}(t)\widetilde{\mathbf{x}}^H(t)]>_c$ and where $< . >_c$ corresponds to the continuous time-averaged operation over an infinite time duration. To solve this problem, the redundancies of $\widetilde{\mathbf{x}}(t)$, appearing for $N > 1$, must be removed and the constraints must be readjusted accordingly. It is proved in [11] that this constrained optimization problem can be transformed to an unconstrained one, by using the following equivalent third-order Volterra GSC structure, for which the redundancies of the observations can be easily withdrawn. Here, $\mathbf{w}_f$ is a $N \times 1$ spatial filter such that $\mathbf{w}_f^H \mathbf{s} = 1$, $\mathbf{B}_{1,0} \stackrel{\text{def}}{=} [\mathbf{u}_1, \ldots, \mathbf{u}_{N-1}]$ where $(\mathbf{s}, \mathbf{u}_1, \ldots, \mathbf{u}_{N-1})$ is an orthogonal basis of $\mathbb{C}^N$, $\widetilde{\mathbf{z}}(t) \stackrel{\text{def}}{=} \mathbf{B}^H \widetilde{\mathbf{x}}(t)$ with $\mathbf{B} \stackrel{\text{def}}{=} \text{Diag}(\mathbf{B}_{1,0}, \mathbf{B}_{1,0}^*, \mathbf{B}_{3,0}, \mathbf{B}_{3,1}, \mathbf{B}_{3,2}, \mathbf{B}_{3,3})$ where $\mathbf{B}_{3,q} \stackrel{\text{def}}{=} \mathbf{B}_{1,0}^{\otimes(3-q)} \otimes \mathbf{B}_{1,0}^{*\otimes q}$, $(0 \le q \le 3)$, $\mathbf{K}$ is the $N_z \times [2(N-1) + 4(N-1)^3]$ selection matrix selecting the non-redundant components of $\widetilde{\mathbf{z}}(t)$, where $N_z = 2(N-1)(2N^2 - N + 3)/3$, $\widetilde{\mathbf{z}}'(t) \stackrel{\text{def}}{=} \mathbf{K}\widetilde{\mathbf{z}}(t)$ and $\widetilde{\mathbf{w}}_{a,\text{opt}}' \stackrel{\text{def}}{=} \arg\{\min_{\widetilde{\mathbf{w}}_a} < E|\mathbf{w}_f^H \mathbf{x}(t) - \widetilde{\mathbf{w}}_a'^H \widetilde{\mathbf{z}}'(t)|^2 >_c\}$ is defined by

$$\widetilde{\mathbf{w}}_{a,\text{opt}}' \stackrel{\text{def}}{=} \left[\mathbf{KB}^H \mathbf{R}_{\widetilde{x}} \mathbf{BK}^H\right]^{-1} \mathbf{KB}^H \mathbf{R}_{\widetilde{x}} \widetilde{\mathbf{w}}_f = \left[\mathbf{KB}^H \mathbf{R}_{\widetilde{n}} \mathbf{BK}^H\right]^{-1} \mathbf{KB}^H \mathbf{R}_{\widetilde{n}} \widetilde{\mathbf{w}}_f, \qquad (4)$$

$\mathbf{R}_{\widetilde{n}} \stackrel{\text{def}}{=} <E[\widetilde{\mathbf{n}}(t)\widetilde{\mathbf{n}}^H(t)]>_c$ and $\widetilde{\mathbf{n}}(t)$ is defined as $\widetilde{\mathbf{x}}(t)$ with $\mathbf{n}(t)$ instead of $\mathbf{x}(t)$. Again, note that for arbitrary L-C$(q_1, q_2, \ldots, q_r)$ or WL-C$(q_1, q_2, \ldots, q_r)$ beamformers, the dimensions of $\widetilde{\mathbf{x}}(t)$, $\mathbf{B}$, $\mathbf{K}$ and $\widetilde{\mathbf{w}}_{a,\text{opt}}'$ must be adjusted accordingly.
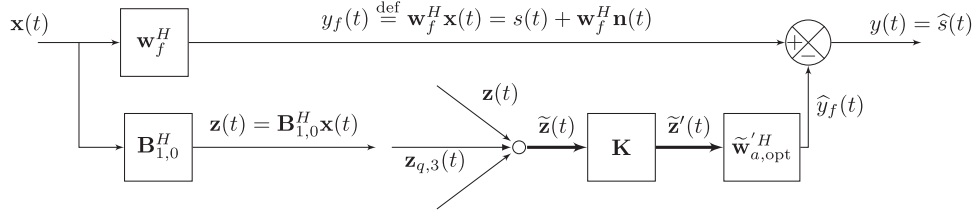
Fig. 1. Equivalent third-order Volterra GSC structure.

2.2.2. Adaptive implementation

One adaptive implementation of $\widetilde{\mathbf{w}}'_{a,\text{opt}}$ may consist in using an extension of the sample matrix inversion (SMI) algorithm [12], i.e., to replace in (4) $\mathbf{R}_{\widetilde{x}}$ by an empirical estimate, $\widehat{\mathbf{R}}_{\widetilde{x}}$, obtained from the K observation snapshots, $\widetilde{\mathbf{x}}(kT_e)$, where T_e is the sample period, and given by

$$\widehat{\mathbf{R}}_{\widetilde{x}} = \frac{1}{K} \sum_{k=1}^{K} \widetilde{\mathbf{x}}(kT_e)\widetilde{\mathbf{x}}^H(kT_e) \overset{\text{def}}{=} <\widetilde{\mathbf{x}}(kT_e)\widetilde{\mathbf{x}}^H(kT_e)>_{d,K}. \tag{5}$$

where $< . >_{d,K}$ corresponds to the discrete time-averaged operation over K samples and where $< . >_{d,+\infty}$ is denoted by $< . >_d$.

2.3. Problem formulation

We consider the observation model (1) for which the interference is digitally and linearly modulated with a symbol period T, arbitrary receive pulse shaping filter $v(t)$ and initial sample time τ. Moreover, we assume that the third-order Volterra MVDR beamformers recalled in Section 2.2 are implemented through the third-order Volterra GSC structure depicted at Fig. 1, where the $\widehat{\mathbf{R}}_{\widetilde{x}}$ matrix (or a part of it for arbitrary L-C$(q_1, q_2, \ldots, q_r)$ or WL-C$(q_1, q_2, \ldots, q_r)$ beamformers) is estimated by $\widehat{\mathbf{R}}_{\widetilde{x}}$ defined by (5). We assume that the interference is potentially oversampled, i.e., that $T_e = T/p$ where p is an integer such that $p \geq 1$. Under these assumptions, the problem which is addressed in this paper consists to analyze the impact on both the steady state (K infinite) and practical (K finite) performance of these beamformers of the parameters $v(t)$, τ and p. For this purpose, three filters $v(t)$, corresponding to a square, a root raised cosine (1/2 Nyquist) and a raised cosine (Nyquist) [13] filters with a roll-off ω are considered, where the square filter is such that $v(t) = 1$ for $-T/2 \leq t \leq T/2$ and $v(t) = 0$ otherwise. Note that the choice in (1) of a square or a 1/2 Nyquist filter $v(t)$ may correspond to a spectrum monitoring context for which the SOI has the pulse shaping filter $v(t)$ and is received through an ideal reception filter around the SOI. Besides, the choice in (1) of a Nyquist filter $v(t)$ may correspond to a radiocommunication context for which the SOI has a 1/2 Nyquist pulse shaping filter and is received through a matched filter to this pulse shaping filter. Note finally that for cycloergodic observations (1) and $p \to \infty$, $<\widetilde{\mathbf{x}}(kT_e)\widetilde{\mathbf{x}}^H(kT_e)>_d \to <\widetilde{\mathbf{x}}(t)\widetilde{\mathbf{x}}^H(t)>_c = <\text{E}[\widetilde{\mathbf{x}}(t)\widetilde{\mathbf{x}}^H(t)]>_c \overset{\text{def}}{=} \mathbf{R}_{\widetilde{x}}$.

3. Asymptotic SO, FO and SIO time-averaged statistics of the interference

Matrix $\mathbf{R}_{\widetilde{n}}$ appearing in (4) contains the continuous time-averaged SO, FO and SIO statistics of the total noise $\widetilde{\mathbf{n}}(t)$. Its estimate, $\widehat{\mathbf{R}}_{\widetilde{n}}$, defined by (5) with $\widetilde{\mathbf{n}}(t)$ instead of $\widetilde{\mathbf{x}}(t)$, contains the discrete time-averaged SO, FO and SIO statistics of $\widetilde{\mathbf{n}}(t)$. For this reason, in order to compute, in Section 4, the steady-state performance of third-order Volterra MVDR beamformers implemented through (5), we compute in this section the normalized asymptotic (K infinite) discrete time-averaged SO, FO and SIO statistics of $\widetilde{\mathbf{n}}(t)$.

These normalized asymptotic statistics correspond to the FO and SIO circular and SO, FO and SIO non-circular coefficients of $j(t)$.

The real-valued FO and SIO circular coefficient of $j(t)$ are simply denoted by $\kappa_{j,c}$ and $\chi_{j,c}$, respectively, defined by

$$\kappa_{j,c} \overset{\text{def}}{=} \frac{<\text{E}|j^4(kT_e)|>_d}{\left(<\text{E}|j^2(kT_e)|>_d\right)^2} \quad \text{and} \quad \chi_{j,c} \overset{\text{def}}{=} \frac{<\text{E}|j^6(kT_e)|>_d}{\left(<\text{E}|j^2(kT_e)|>_d\right)^3}. \tag{6}$$

The generally complex-valued SO, FO and SIO non-circular coefficients of $j(t)$ are simply denoted by γ_j, $\kappa_{j,nc,i}$ and $\chi_{j,nc,i}$, respectively, defined by

$$\gamma_j \overset{\text{def}}{=} \frac{<\text{E}[j^2(kT_e)]>_d}{<\text{E}|j^2(kT_e)|>_d}, \tag{7}$$

$$\kappa_{j,nc,i} \overset{\text{def}}{=} \frac{<\text{E}[j^{5-i}(kT_e)j^{*(i-1)}(kT_e)]>_d}{\left(<\text{E}|j^2(kT_e)|>_d\right)^2}, i = 1, 2, \quad \text{and}$$

$$\chi_{j,nc,i} \overset{\text{def}}{=} \frac{<\text{E}[j^{7-i}(kT_e)j^{*(i-1)}(kT_e)]>_d}{\left(<\text{E}|j^2(kT_e)|>_d\right)^3}, i = 1, 2, 3. \tag{8}$$

Using the definition of $j(t)$ in (1) into (6)–(8), we obtain:

$$\gamma_j = e^{i2\phi}\gamma_a, \tag{9}$$

$$\kappa_{j,c} = \kappa_{a,c}r_{v,1} + \left(2 + |\gamma_a^2|\right)r_{v,2}, \tag{10}$$

$$\kappa_{j,nc,1} = e^{i4\phi}\left(\kappa_{a,nc,1}r_{v,1} + 3\gamma_a^2 r_{v,2}\right),$$
$$\kappa_{j,nc,2} = e^{i2\phi}\left(\kappa_{a,nc,2}r_{v,1} + 3\gamma_a r_{v,2}\right), \tag{11}$$

$$\chi_{j,c} = \chi_{a,c}r_{v,3} + \left(3\gamma_a\kappa_{a,nc,2}^* + 9\kappa_{a,c} + 3\gamma_a^*\kappa_{a,nc,2}\right)r_{v,4} + \left(9|\gamma_a^2| + 6\right)r_{v,5}, \tag{12}$$

$$\chi_{j,nc,1} = e^{i6\phi}\left(\chi_{a,nc,1}r_{v,3} + 15\gamma_a\kappa_{a,nc,1}r_{v,4} + 15\gamma_a^3 r_{v,5}\right), \tag{13}$$

$$\chi_{j,nc,2} = e^{i4\phi}\left[\chi_{a,nc,2}r_{v,3} + (10\gamma_a\kappa_{a,nc,2} + 5\kappa_{a,nc,1})r_{v,4} + 15\gamma_a^2 r_{v,5}\right], \tag{14}$$

$$\chi_{j,nc,3} = e^{i2\phi}\left[\chi_{a,nc,3}r_{v,3} + (6\gamma_a\kappa_{a,c} + 8\kappa_{a,nc,2} + \gamma_a^*\kappa_{a,nc,1})r_{v,4} + 3\gamma_a\left(|\gamma_a^2| + 4\right)r_{v,5}\right]. \tag{15}$$

Here γ_a, $\kappa_{a,c}$, $\kappa_{a,nc,1}$, $\kappa_{a,nc,2}$, $\chi_{a,c}$, $\chi_{a,nc,1}$, $\chi_{a,nc,2}$ and $\chi_{a,nc,3}$ are the SO, FO and SIO coefficients of the symbol a_n whereas the coefficients $r_{v,j}$, $j = 1, \ldots, 5$ are defined by:

$$r_{v,1} \overset{\text{def}}{=} \frac{\frac{1}{p}\sum_{i=0}^{p-1}\sum_k v_{k,i,\tau}^4}{\left[\frac{1}{p}\sum_{i=0}^{p-1}\sum_k v_{k,i,\tau}^2\right]^2}, \quad r_{v,2} \overset{\text{def}}{=} \frac{\frac{1}{p}\sum_{i=0}^{p-1}\sum_{k \neq \ell} v_{k,i,\tau}^2 v_{\ell,i,\tau}^2}{\left[\frac{1}{p}\sum_{i=0}^{p-1}\sum_k v_{k,i,\tau}^2\right]^2}, \tag{16}$$

$$r_{v,3} \stackrel{\text{def}}{=} \frac{\frac{1}{p}\sum_{i=0}^{p-1}\sum_k \nu_{k,i,\tau}^6}{\left[\frac{1}{p}\sum_{i=0}^{p-1}\sum_k \nu_{k,i,\tau}^2\right]^3}, \quad r_{v,4}\stackrel{\text{def}}{=}\frac{\frac{1}{p}\sum_{i=0}^{p-1}\sum_{k\neq\ell} \nu_{k,i,\tau}^4 \nu_{\ell,i,\tau}^2}{\left[\frac{1}{p}\sum_{i=0}^{p-1}\sum_k \nu_{k,i,\tau}^2\right]^3}, \quad (17)$$

$$r_{v,5} \stackrel{\text{def}}{=} \frac{\frac{1}{p}\sum_{i=0}^{p-1}\sum_{k\neq\ell,\ell\neq m,m\neq k} \nu_{k,i,\tau}^2 \nu_{\ell,i,\tau}^2 \nu_{m,i,\tau}^2}{\left[\frac{1}{p}\sum_{i=0}^{p-1}\sum_k \nu_{k,i,\tau}^2\right]^3}, \quad (18)$$

where $\nu_{k,i,\tau} \stackrel{\text{def}}{=} \nu(kT + iT/p - \tau)$. Note that when the oversampling factor p tends to infinite, the discrete time-averaged operation becomes equivalent to a continuous time-averaged operation and (16)–(18) become:

$$r_{v,1} = \frac{\overline{\nu^4(t)}}{\left[\overline{\nu^2(t)}\right]^2}, \quad r_{v,2} = \frac{2\sum_{k=1}^\infty \overline{\nu^2(t)\nu^2(t-kT)}}{\left[\overline{\nu^2(t)}\right]^2}, \quad (19)$$

$$r_{v,3} = \frac{\overline{\nu^6(t)}}{\left[\overline{\nu^2(t)}\right]^3}, \quad r_{v,4} = \frac{\sum_{k\neq 0}\overline{\nu^4(t)\nu^2(t-kT)}}{\left[\overline{\nu^2(t)}\right]^3}, \quad r_{v,5}$$

$$= \frac{\sum_{k\neq\ell,k\neq 0,\ell\neq 0}\overline{\nu^2(t)\nu^2(t-kT)\nu^2(t-\ell T)}}{\left[\overline{\nu^2(t)}\right]^3}, \quad (20)$$

where $\overline{(.)} \stackrel{\text{def}}{=} \frac{1}{T}\int_{-\infty}^{+\infty}(.)dt$. Expressions (10)–(15), which are completely new, show that, in general, the filter $\nu(t)$ modifies the FO and SIO coefficients of the symbol a_k. However, in the particular case of a filter $\nu(t)$ which is rectangular over the symbol duration T, it is easy to verify that $r_{v,1} = r_{v,3} = 1$ and $r_{v,2} = r_{v,4} = r_{v,5} = 0$, which means that coefficients of $j(t)$ and $e^{i\phi}a_k$ coincide both at FO and SIO. Such a situation also occurs when $\nu(t)$ is a Nyquist filter provided that the observations are optimally sampled, i.e., that $p = 1$ and $\tau = 0$.

4. Impact of the pulse-shaping filter on the steady state performance

4.1. Steady-state performance of the third-order Volterra MVDR beamformers

From Fig. 1, it is straightforward to compute the ratio of the asymptotic discrete time-averaged powers of the SOI and the total noise at the output, $y(t)$, of the third-order Volterra MVDR beamformers, referred to as the output SINR. This output SINR is given by Chevalier et al. [11]:

$$\text{SINR}_{\text{MVDR}} = \frac{\pi_s}{\mathbf{w}_f^H\left[\mathbf{R}_n - \mathbf{R}_{\tilde{n},n}^H\mathbf{B}\mathbf{K}^H(\mathbf{K}\mathbf{B}^H\mathbf{R}_{\tilde{n}}\mathbf{B}\mathbf{K}^H)^{-1}\mathbf{K}\mathbf{B}^H\mathbf{R}_{\tilde{n},n}\right]\mathbf{w}_f}, \quad (21)$$

where $\mathbf{R}_{\tilde{n},n} \stackrel{\text{def}}{=} <E[\tilde{\mathbf{n}}(kT_e)\tilde{\mathbf{n}}^H(kT_e)]>_d$ and $\pi_s \stackrel{\text{def}}{=} <E|s^2(kT_e)|>_d$. Expression (21) adjusted accordingly at the output of the L-C(q) MVDR beamformers, ($0 \leq q \leq 3$), has been developed in [11] for $N = 2$ and the model (1) and has been proved to be given by:

$$\text{SINR}_{LC(q)} = \epsilon_s\frac{\left(1 + \epsilon_j\beta^2\right)A_q}{\left(1 + \epsilon_j\right)A_q - \alpha^2\beta^6\epsilon_j^4 D_q}. \quad (22)$$

Here, $\epsilon_s \stackrel{\text{def}}{=} \|\mathbf{s}\|^2\pi_s/\eta_2$, $\epsilon_j \stackrel{\text{def}}{=} \|\mathbf{j}\|^2\pi_j/\eta_2$ with $\pi_j \stackrel{\text{def}}{=} <E|j^2(kT_e)|>_d$, η_2 is the background noise power per sensor, $\alpha \stackrel{\text{def}}{=} |\mathbf{s}^H\mathbf{j}|/\|\mathbf{s}\|\|\mathbf{j}\|$ and $\beta \stackrel{\text{def}}{=} \sqrt{1 - \alpha^2}$ and where the quantities A_q and D_q, $q = 0,\ldots,3$ are defined by

$$A_0 = A_2 \stackrel{\text{def}}{=} \beta^8\epsilon_j^4\left(\chi_{j,c} - |\kappa_{j,nc,2}^2|\right) + \beta^6\epsilon_j^3\left(\chi_{j,c} + 9\kappa_{j,c} - 6\text{Re}\left(\gamma_j\kappa_{j,nc,2}^*\right)\right)$$
$$+ 9\beta^4\epsilon_j^2\left(\kappa_{j,c} + 2 - |\gamma_j^2|\right) + 24\beta^2\epsilon_j + 6, \quad (23)$$

$$A_1 \stackrel{\text{def}}{=} \beta^8\epsilon_j^4\left(\chi_{j,c} - \kappa_{j,c}^2\right) + \beta^6\epsilon_j^3\left(\chi_{j,c} + \kappa_{j,c}\right)$$
$$+ \beta^4\epsilon_j^2\left(5\kappa_{j,c} + 2\right) + 8\beta^2\epsilon_j + 2, \quad (24)$$

$$A_3 \stackrel{\text{def}}{=} \beta^8\epsilon_j^4\left(\chi_{j,c} - |\kappa_{j,nc,1}^2|\right) + \beta^6\epsilon_j^3\left(\chi_{j,c} + 9\kappa_{j,c}\right)$$
$$+ 9\beta^4\epsilon_j^2\left(\kappa_{j,c} + 2\right) + 24\beta^2\epsilon_j + 6, \quad (25)$$

$$D_0 \stackrel{\text{def}}{=} |\kappa_{j,nc,2} - 3\gamma_j|^2; \quad D_1 \stackrel{\text{def}}{=} (\kappa_{j,c} - 2)^2; \quad (26)$$

$$D_2 \stackrel{\text{def}}{=} |(\kappa_{j,nc,2} - \gamma_j) + 2\gamma_j/(\beta^2\epsilon_j)|^2; \quad D_3 \stackrel{\text{def}}{=} |\kappa_{j,nc,1}^2|. \quad (27)$$

Defining the SINR gain with respect to the Capon beamformer, $G_B \stackrel{\text{def}}{=} \text{SINR}_B/\text{SINR}_L$, obtained in using the beamformer B instead of Capon beamformer, where $\text{SINR}_L = \epsilon_s[1 - \alpha^2\epsilon_j/(1 + \epsilon_j)]$, we obtain [11]:

$$G_{L-C(q)} = 1 + \frac{\alpha^2\beta^6\epsilon_j^4 D_q}{(1 + \epsilon_j)A_q - \alpha^2\beta^6\epsilon_j^4 D_q}, \quad (28)$$

Expressions (22) and (28), with (23) to (27), allow us to specify how the L-C(q) MVDR beamformers outperform the Capon beamformer for circular and non-circular non-Gaussian interference, depending on both ϵ_j and the normalized SO, FO and SIO interference statistics. For $q = 0,1,2,3$, it has been shown in particular in [11] that a necessary condition to obtain substantial performance gain at the output of the L-C(q) MVDR beamformer is to cancel the dominant terms in ϵ_j of A_q. This occurs for interference such that $\chi_{j,c} - |\kappa_{j,nc,2}^2| = 0$, ($q = 0,2$), $\chi_{j,c} - \kappa_{j,c}^2 = 0$, ($q = 1$) and $\chi_{j,c} - |\kappa_{j,nc,1}^2| = 0$, ($q = 3$), which corresponds for example to BPSK ($q = 0,2$), PSK ($q = 1$) and QPSK ($q = 3$) interference with a square pulse shaping filter respectively. However, when the pulse shaping filter of the interference is no longer square, the dominant terms in ϵ_j of A_q is no longer zero and one may then wonder what may be the impact on performance of $\nu(t)$, p and τ. The latter may be analyzed for L-C(q) MVDR beamformers in particular using (9) to (18) into (22) and (28).

4.2. Impact of $\nu(t)$, p and τ on the output SINR of the third-order Volterra MVDR beamformer

In order to analyze the impact on the output SINR of parameters $\nu(t)$, p and τ, we consider a two-element array with unit gain sensors and we assume that the SOI has a signal to noise ratio (SNR), π_s/η_2, equal to 10 dB. This SOI is assumed to be corrupted by an interference (model (1)) whose INR, π_j/η_2, is equal to 30 dB. Under these assumptions, Fig. 2 displays, for a BPSK interference, for $\tau = 0$, for three pulse shaping filters $\nu(t)$ corresponding to a square, a 1/2 Nyquist and a Nyquist filter with a roll-off $\omega = 0.3$, and for $p = 1$ (sampling at one sample per symbol) and $p = +\infty$ (continuous-time observation), the variations of $G_{L-C(0)}$ at the output of the L-C(0) MVDR beamformer as a function of α. In a similar way,[1] Fig. 3 displays, under the same assumptions as Fig. 2, the variations of $G_{L-C(1,3)}$ at the output of the L-C(1,3) MVDR beamformer as a function of α but for a QPSK interference. Note for high values of α not equal to one, high values of $G_{L-C(0)}$ and $G_{L-C(1,3)}$ for the square (whatever the value of p) and the Nyquist (for $p = 1$) filters, due to the absence of interference intersymbol interference (ISI) at reception but low values of $G_{L-C(0)}$ and $G_{L-C(1,3)}$ for both the Nyquist filter (for $p = +\infty$) and the 1/2 Nyquist filter

---

[1] The analytical expressions of $G_{L-C(1,3)}$ for a QPSK interference and $G_{L-C(0)}$ for a BPSK interference are identical for a square filter but otherwise they are different, but numerically very close.
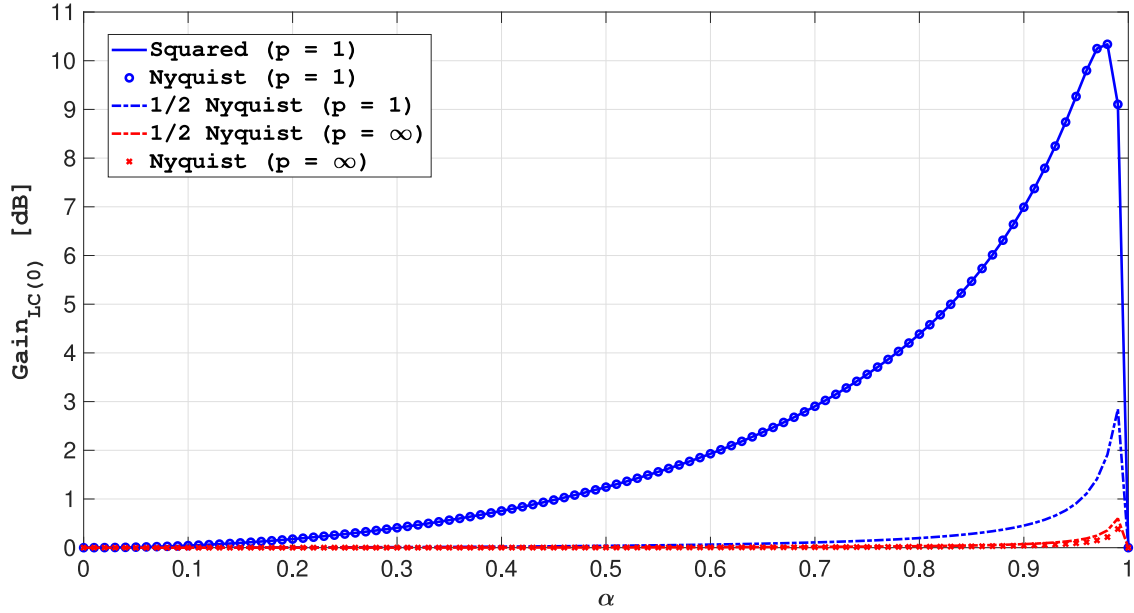
Fig. 2. $G_{L\text{-}C(0)}$ as a function of α for $N = 2$, SNR = 10 dB, INR = 30 dB, BPSK interference and $(\omega, \tau) = (0.3, 0)$.

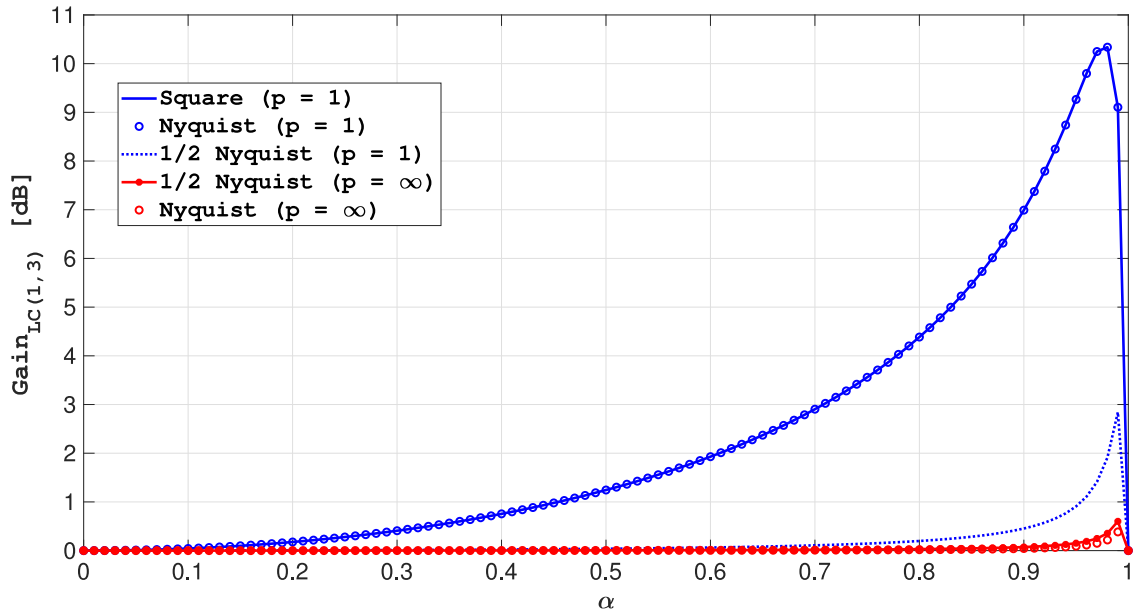**Fig. 3.** $G_{L\text{-}C(1,3)}$ as a function of α for $N = 2$, SNR = 10 dB, INR = 30 dB, QPSK interference and $(\omega, \tau) = (0.3, 0)$.

(whatever the value of p) due to the presence of interference ISI at reception. Note, in this latter case, the decreasing performance gain as p increases from 1 to infinite. Note that the previous results for 1/2 Nyquist and Nyquist filters are maintained whatever the value of the roll-off factor ω, provided that $\tau = 0$. These results show the very high sensitivity of the third-order Volterra MVDR beamformers [11] to both the interference pulse shaping filter and oversampling factor p (for a non square pulse shaping filter). Indeed, these parameters highly modify the FO and SIO interference statistics, which prevent conditions $\chi_{j,c} - \kappa_{j,c}^2 = 0$ and $\chi_{j,c} - |\kappa_{j,nc,1}^2| = 0$ to remain valid.

To complete these results, Fig. 4 analyzes the effect on the performance of the initial sampling time τ by showing, in the same context as Fig. 3, the variations of $G_{L\text{-}C(1,3)}$ as a function of τ/T for $p = 1$ and $p = 2$ and for $\alpha = 0.95$. We note high values of

$G_{L\text{-}C(1,3)}$ for the square filter, whatever the value of τ, and for the Nyquist filter for $(p, \tau) = (1, 0)$, due to the absence of interference ISI at reception. However, we note low values of $G_{L\text{-}C(1,3)}$ for the 1/2 Nyquist filter, whatever the value of τ, and for the Nyquist filter for $(p, \tau) \neq (1, 0)$, due to the presence of interference ISI at reception. Similar results would be obtained for other values of $(p, \tau) \neq (1, 0)$ and other third-order Volterra MVDR beamformers. These results show the weak robustness of the third-order Volterra MVDR beamformers with respect to the initial sampling time for a non-square pulse shaping filter. As a summary, for digitally and linearly modulated interference, the results of this section show the weak robustness of the third-order Volterra MVDR beamformers to the presence interference ISI at reception, and thus, for non-square pulse shaping filter of the interference, the very high sensitivity of these beamformers to both the initial sample time,
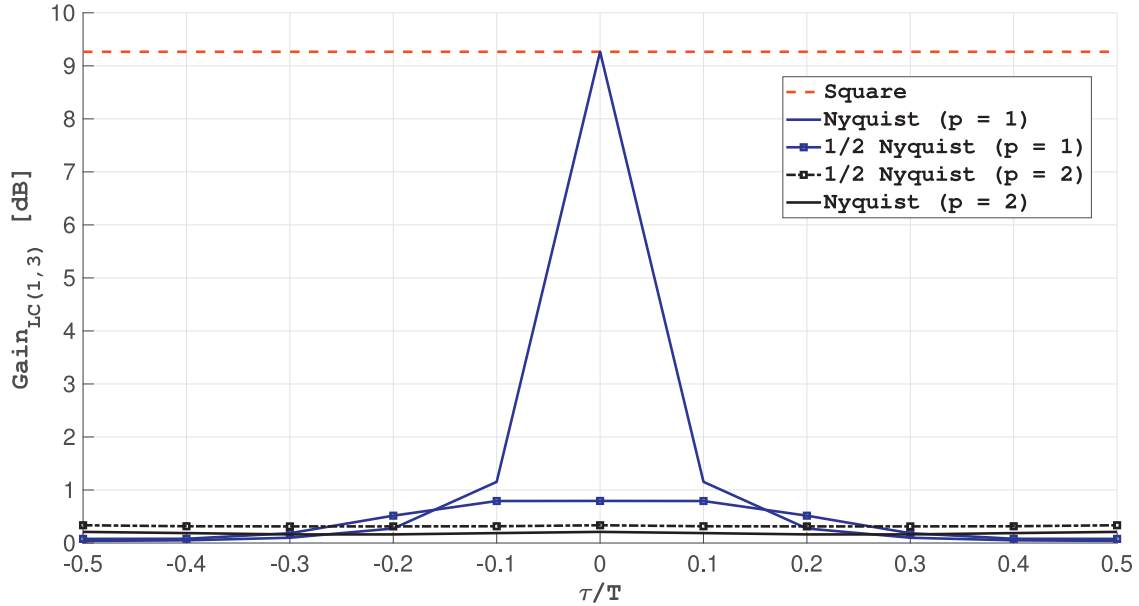
Fig. 4. $G_{L-C(1,3)}$ as a function of τ/T for $N = 2$, SNR = 10 dB, INR = 30 dB, QPSK interference and $(\omega, \alpha) = (0.3, 0.95)$.

the oversampling and the kind of filter, which modify the FO and SIO statistics of the interference.

5. Impact of the pulse-shape filter on the finite sample performance

5.1. Finite sample performance of the third-order Volterra MVDR beamformers

When $\mathbf{R}_{\tilde{x}}$ is estimated from K samples by (5), the SINR at the output of the third-order Volterra beamformers becomes [11]:

$$\text{SINR}(K) = \frac{\pi_s}{\left(\widetilde{\mathbf{w}}_f - \mathbf{B}\widehat{\widetilde{\mathbf{w}}}'_{a,\text{opt}}\right)^H \mathbf{R}_{\tilde{x}}\left(\widetilde{\mathbf{w}}_f - \mathbf{B}\widehat{\widetilde{\mathbf{w}}}'_{a,\text{opt}}\right) - \pi_s}, \qquad (29)$$

where $\widetilde{\mathbf{w}}_f \overset{\text{def}}{=} [\mathbf{w}_f^T, \mathbf{0}_{N+4N^3}^T]^T$ and $\widehat{\widetilde{\mathbf{w}}}'_{a,\text{opt}}$ is defined by (4) with $\widehat{\mathbf{R}}_{\tilde{x}}$ instead of $\mathbf{R}_{\tilde{x}}$.

5.2. Impact of v(t), p and τ on SINR(K) at the output of the third-order Volterra beamformers

In order to analyze the impact on the output SINR(K) of parameters $v(t)$, p and τ, we consider the same scenario as Fig. 4. Under these assumptions, Fig. 5 displays, for the three pulse shaping filters $v(t)$ corresponding to a square, a 1/2 Nyquist and a Nyquist filter with a roll-off $\omega = 0.3$, and for $(p, \tau) = (1, 0)$, the variations of the estimated mean value of $G_{L-C(1,3)}(K) \overset{\text{def}}{=}$ SINR$_{L-C(1,3)}(K)/$SINR$_L$, $\widehat{E}(G_{L-C(1,3)}(K))$, computed over 1000 runs, at the output of the L-C(1, 3) MVDR beamformers as a function of K. Note again, for sufficient values of K, a high value of $\widehat{E}(G_{L-C(1,3)}(K))$
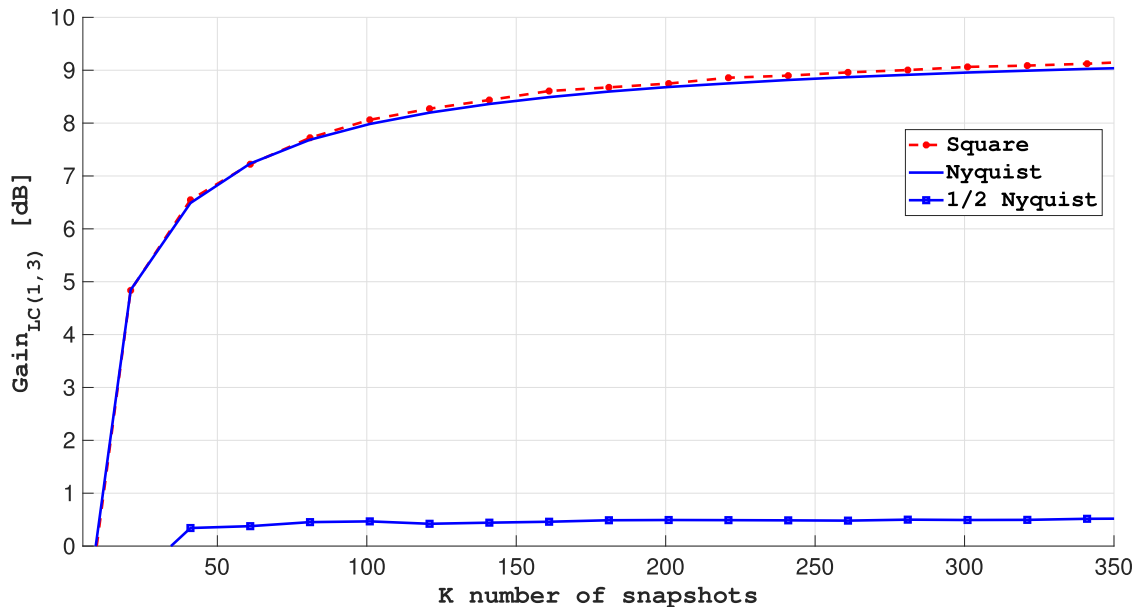

Fig. 5. $\widehat{E}(G_{L-C(1,3)}(K))$ as a function of K for $N = 2$, SNR = 10 dB, INR = 30 dB, $\alpha = 0.95$, 1000 runs, QPSK interference, $(p, \tau) = (1, 0)$.

for the square and Nyquist filters, due to the absence of interference ISI at reception, but low values of $\widehat{E}(G_{L\text{-}C(1,3)}(K))$ for the 1/2 Nyquist filter due to the presence of interference ISI at reception in this case. This confirms the results of section IV.

6. Conclusion

A sensitivity analysis of recently proposed third-order Volterra MVDR beamformers to both pulse shaping filter, oversampling and initial sample time of interference has been presented in this paper. It has been shown that the high performance gain values with respect to Capon obtained for some linearly and digitally modulated interference having a receive square pulse shaping filter [11] are lost for non-square pulse shaping filter generating ISI at reception. This occurs for non-Nyquist filter, for an oversampling reception or when the initial sampling time is not optimal. Technics to robustify the third-order Volterra MVDR beamformers [11] to the previous interference parameters are then required and remain to be developed. The exploitation of spatio-temporal structures of beamforming may be a direction of investigation.

Declaration of Competing Interest

We have no conflict of interest in this article submitted.

References

[1] B.D.V. Veen, K.M. Buckley, Beamforming: a versatile approach to spatial filtering, in: IEEE ASSP Magazine, 1988, pp. 4–24.
[2] J. Capon, R.J. Greenfield, R.J. Kolker, Multidimensional maximum likelihood processing of a large aperture seismic array, Proc. IEEE 55 (2) (1967) 191–211.
[3] O.L. Frost III, An algorithm for linearly constrained adaptive array processing, Proc. IEEE 60 (8) (1972) 926–935.
[4] L.J. Griffiths, C.W. Jim, An alternative approach to linearly constrained adaptive beamforming, IEEE Trans. Ant. Prop. AP-30 (1) (1982) 27–34.
[5] B. Picinbono, P. Chevalier, Widely linear estimation with complex data, IEEE Trans. Signal Process. 43 (8) (1995) 2030–2033.
[6] B. Picinbono, On circularity, IEEE Trans. Signal Process. 42 (12) (1994) 3473–3482.
[7] P. Chevalier, A. Blin, Widely linear MVDR beamformer for the reception of an unknown signal corrupted by noncircular interferences, IEEE Trans. Signal Process. 55 (11) (2007) 5323–5336.
[8] P. Chevalier, J.P. Delmas, A. Oukaci, Optimal widely linear MVDR beamforming for noncircular signals, in: Proc. ICASSP, Taipei (Taiwan), 2009.
[9] P. Chevalier, J.P. Delmas, A. Oukaci, Properties, performance and practical interest of the widely linear MMSE beamformer for nonrectilinear signals, Signal Process. Elsevier 97 (2014) 269–281.
[10] P. Chevalier, F. Pipon, New insights into optimal widely linear array receivers for the demodulation of BPSK, MSK and GMSK signals corrupted by non circular interferences - application to SAIC, IEEE Trans. Signal Process. 54 (3) (2006) 870–883.
[11] P. Chevalier, J.P. Delmas, M. Sadok, Third-order Volterra MVDR beamforming for non-gaussian and potentially non-circular interference cancellation, IEEE Trans. Signal Process. 66 (18) (2018) 4766–4781.
[12] I.S. Reed, J.D. Mallet, L.E. Brennan, Rapid convergence rate in adaptive arrays, IEEE Trans. Aerosp. Electron. Syst. 10 (6) (1974) 853–863.
[13] G.J. Proakis, Digital Communications, Series in Electrical and Computation Engineering, fourth ed., Mc Graw Hill, 2001.